Mon. Not. R. Astron. Soc. **279,** 293–300 (1996)

Star/galaxy classification using Kohonen self-organizing maps

A. S. Miller★ and M. J. Coe

Physics Department, The University, Southampton, SO17 1BJ

Accepted 1995 October 10. Received 1995 October 9; in original form 1995 June 5

ABSTRACT

The automatic classification of star/galaxy data sets is of growing importance as the size of survey data sets increases. Here we present a classifier based on the Kohonen self-organizing map (SOM). The SOM was trained to classify by type using only a small number of manually classified objects. Galaxy classification accuracies of 98 per cent are achieved for objects with a limiting magnitude of 20.

Key words: methods: data analysis – techniques: image processing – astronomical data bases: miscellaneous – catalogues – surveys – stars: general.

1 INTRODUCTION

The construction of galactic catalogues has occupied astronomers for over two centuries. The first, Messier's catalogue of nebulous objects, dates back to 1784. The first *complete* survey of extragalactic nebulae, containing over 11 000 objects, was published by Charlier (1922). This made readily apparent the inhomogeneity in the distribution of galaxies. Since then surveys have increased in size by several orders of magnitude. The amount of information requiring processing has also increased due to the introduction of surveys which utilize galaxy redshifts to provide distance estimates, allowing the construction of 3D population distributions.

The galaxy populations at early epochs of the Universe are an important cosmological probe. The use of deep all-sky and selected-area surveys to provide accurate population distributions now forms an important part of modern cosmological research. By looking at ever fainter populations of galaxies it is possible to chart the clustering and evolution of galaxies back to an epoch 40 per cent of the time since the Universe was formed in the big bang. The population distribution of galaxies to a magnitude of 24 shows an excess when compared to a population model which assumes no galactic luminosity evolution (Ellis 1987). It was suggested that a large portion of the 20–40 per cent excess at $B \sim 21$–22 can be attributed to a 5 per cent population excess of faint blue galaxies at $B \sim 17$ (Kron 1982). Subsequent redshift surveys have shown that these blue galaxies are, in fact, not at high redshifts, but faint galaxies which have decreased in number by today, possibly by mergers with other galaxies (Broadhurst, Ellis & Shanks 1988). Fainter surveys are required to clarify the excess population anomaly.

Selection of stellar, or stellar-like objects, such as quasars (quasi-stellar objects), is equally important (Boyle 1991). By removing galaxies and local Galactic stars from surveys, a list of quasar candidates can be created. Their high luminosities make them observable at very large distances, at redshifts $z > 3$, when the Universe was 20 per cent of its present age. Clustering and density of these objects in the early Universe can be used to place constraints on methods of galaxy formation.

Cosmologists have therefore continued to create all-sky and regional surveys of ever increasing sensitivity. Some of the deepest galaxy catalogues, such as those of the Edinburgh–Durham survey (Heydon-Dumbleton, Collins & MacGillivray 1989), the APM galaxy survey (Maddox et al. 1990), Zwicky et al. (1961–68) and Corwin, de Vaucouleurs & de Vaucouleurs (1985), have relied on the visual inspection of photographic plates to classify objects. The size of such surveys is now forcing astronomers to turn to automated classification methods, as manual classification is both impractical and too subjective. The Second Palomar Observatory Sky Survey (POSS-II) survey is expected to comprise of 900 plates and contain of the order of 2×10^8 objects, and amounts to close to two terabytes of data (Weir et al. 1992). There is no reason to expect this growth in survey size to be reduced. Astronomers must therefore now address the data analysis problems that they will face in the 21st century.

Within the last decade artificial intelligence (AI) research has started to produce sophisticated techniques which have provided novel solutions to some object classification problems. Artificial neural networks (ANNs), an AI paradigm first investigated in the 1940s, has undergone a renaissance.

★E-mail: asm@npac.syr.edu

An investigation into the applicability of back-propagation neural networks to the star/galaxy classification problem has already been undertaken (Odewahn et al. 1992; Odewahn & Nielson 1994). The use of neural networks and related techniques for telescope plate object classification and other problems related to astronomy are discussed elsewhere (Miller 1993; Lahav 1994; Serra-Ricart, Garrido & Gaitan 1994). Other, more conventional, techniques are reviewed by Heydon-Dumbleton et al. (1989).

2 UNSUPERVISED LEARNING AND KOHONEN MAPS

The majority of work in the application of ANNs has focused on the use of the back-propagation algorithm of Rumelhart, Hinton & McClelland (1986). Other forms of neural network have been developed, each with specific strengths and weaknesses (Widrow & Lehr 1990). The Kohonen map, an unsupervised learning technique, is considered here.

Unsupervised learning, as employed by the networks of Hopfield & Tank (1986), Kohonen (1990) and others, require no exemplar outputs. A self-organizing map (SOM) simply consists of input and hidden neurons. The network learns by associating different input pattern types with different clusters of hidden nodes. When trained, different groups of hidden neurons respond to different classes of input patterns.

A Kohonen SOM classifier was used for the image characterization task. Further C code and UNIX shell scripts were developed by the authors to process the POSS II/APS files and the SOM output. The network was trained using a set of example objects. These objects, like all those in the data set, were classified as stars or galaxies. During training, however, the SOM did not use the classification type for weight modification, only the object parameters. Objects were therefore clustered by the similarity to each other in the input parameter space.

A subset of the training data was then used for map calibration. During this phase each object in the calibration set was presented to the map. The node which closest matches each object is then classified as representing that object type. If a node is matched by more than one object, the one with the lowest error has its type associated with the node. The ability to use a calibration set which is smaller than the training set reduces the number of objects which must be classified for training. A back-propagation network would require all 6000 objects to be classified for training. The SOM requires a few hundred manually classified objects and achieves a similar classification performance.

3 THE STAR/GALAXY DATA SET

The star/galaxy data set used here was created by Odewahn et al. (1992) using the Automated Plate Scanner (APS) at the University of Minnesota. The data set consists of 5528 stars and 3717 galaxies, a total of 9245 objects. The APS was used to scan a single POSS O-band plate (B mag), P323, which contains the Coma cluster of galaxies. The scanner records plate transmission values above a certain density, relative to the local sky background level, corresponding to 23.5 B-mag arcsec^{-2} for the current POSS survey. The transmission values are used, rather than the intensities, to reduce the plate processing time. Odewahn et al. classified selected areas of the plate by visual inspection and the use of the deep galaxy catalogue of the Coma cluster (Godwin, Metcalfe & Peach 1983).

The objects which form the data set were obtained from three regions of the POSS plate. Region 1 contains the core of the Coma cluster. Galaxies were selected by correlating object positions with galaxy catalogue of Godwin et al. (1983). Stars were selected by identifying plate objects which did not appear in the galactic catalogue and with a diameter greater than 40 μm. Objects in region 2 were classified as stars and galaxies by visual inspection of a selected sample of objects with a limiting diameter of 40 μm. Region 3 comprises all objects within a specified plate area with a limiting diameter of 73 μm. In this case, objects were classified by visual inspection as stars, galaxies, merged stellar objects, plate defects and uncertain types. The data set used here includes only the star and galaxy objects in region 3; plate defects are not considered.

Visual classification of objects involved the removal of plate defects and merged images. A set of *conservative* selection rules, which minimized the number of contaminating objects in each class, were then used to separate objects in D–T_{av}, D–T_c and m–T_{av} parameter spaces (Odewahn & Nielson 1994), where D is the object diameter, T_{av} and T_c are the average and central transmissions, and m is the first moment of transmission weighted to $1/r$. Finally, each object was inspected visually, and excluded if incorrect. A few more faint contaminating objects were also rejected after the classifier developed by Odewahn & Neilson failed to classify them correctly, and further visual inspection showed them to be borderline cases. It should be emphasized that the majority of objects incorrectly classified by Odewahn & Neilson's classifier remain in the data set.

The objects were divided into training and testing data according to their location on the POSS plate (Table 1).

Each object scanned from the POSS plate is characterized by 14 APS parameters: major-axis diameter (D), ellipticity (E), average transmission over the image (T_{av}), central image transmission (T_c), ratio of area of circle with semi-major axis radius to actual area (c_1), log of the actual area (c_2), transmission momentum weighted to $1/r(m)$, rms error of ellipse fit to image transit end points (f), Y centroid error (j), image gradients ($g_{14}, g_{13}, g_{12}, g_{23}$ and g_{34}). In addition, two more parameters were defined from the 14 obtained from the POSS plate: $T_r(=T_{av}/T_c)$ and $T_{cA}(=T_c/\sqrt{A})$; these parameters were included because they are frequently using in classifications (Heydon-Dumbleton et al. 1989).

The data set contains small populations of objects at both extremes of the diameter range. No classifier developed using this data set could be expected to perform well for objects below 70 μm or above 350 μm, due to the very low

Table 1. Objects in the 40–330 μm diameter range by region.

Region:	Stars	Galaxies	Total
1 & 2, training	3390	2741	6335
3, testing	2119	756	2920

number of examples available to form both training and test sets. In addition, stellar objects with diameters greater than 330 μm exhibit diffraction spikes, which cause them to appear as extended (galaxy-like) objects in the POSS parameter space. A classifier was therefore developed taking these data set features into account. Only objects in the 70–330 μm diameter range were considered.

Assuming a random error (Poisson distribution) in the classification of test-region objects, classification errors for the whole data set of 3.6 per cent for galaxies and 2.2 per cent for stars would be expected. However, the low number of objects, notably galaxies, with diameters greater than 230 μm may lead to greater statistical noise in the classification results. As already discussed, expected errors for the overall classification rates are of the order of a few per cent. When the test data are split into diameter ranges of 20 μm, each band contains at most about 10^2 objects, suggesting much larger errors of around 10 per cent for classification accuracy in a given diameter band.

It is important to establish the limiting magnitude of any classification technique, because the population of faint objects is of most interest to astronomers. As the absolute magnitudes of the objects are not known, and accurate magnitudes are not required to establish the classifier's overall performance, object diameters may be related to magnitudes using simple magnitude–diameter relationships. The stellar relation was fitted using sequences from CCD images and has an rms scatter of 0.15–0.20 mag. The galaxy relation used 1500 galaxies from the Coma cluster survey (Godwin et al. 1983) having a scatter of 0.3 mag. The minimum object diameter of 70 μm implies that the limiting magnitudes of the data set are 20.3 for stars (M_s) and 20.7 for galaxies (M_g). Very bright objects with diameters greater than 330 μm ($M_s < 16.0$, $M_g < 12.3$) are also excluded.

4 THE IDEAL STAR/GALAXY CLASSIFIER

For cosmological purposes, it is the separation of the galaxy population that is of interest to the astronomer. Thus two additional terms are defined.

(1) Completeness is defined as the percentage of galaxies which are correctly identified.
(2) Contamination is the percentage of stars which become classified as part of the galaxy sample.

An ideal classifier would have 100 per cent completeness with zero per cent contamination. As we shall see later, there is a trade-off between completeness and contamination.

5 MAP DATA PRESENTATION AND OPTIMIZATION

Presenting raw data to a neural network is rarely the most efficient method of parameter input; data set normalization is thought to improve the classification performance (Hancock 1988; Kohonen, Kangas & Laaksonen 1992). The APS parameters vary over vastly differing ranges and in some cases take different units. SOMs, like principal component analysis (Joliffe 1986), are also sensitive to parameter scale (Kohonen et al. 1992). Each input parameter was rescaled by subtracting the mean and dividing by the parameter variance, thus making them scale-independent. Any such scheme is arbitrary, especially if input parameters take different units, as they do in this case, where the input parameters vary over a range of 0.0–0.93 for ellipticity (E) to 2688–4095 for central image transmission (T_c). The following two strategies were used:

(1) using the raw data as input to the network, and
(2) using normalized data as inputs to the network, the normalization coefficients being calculated from the whole of the training set over the full diameter range (70–330 μm). Each parameter was normalized by subtracting the mean and dividing by the variance. The normalized data set was then used to train maps with two sets of input parameters:

(i) the standard 14 APS object parameters, and
(ii) a fuller set of 16 object parameters, the APS parameters with two additional ones derived from them: $T_r = (T_{av}/T_c)$ and $T_{cA} = (T_c/A)$, where A is the object area (derived from c_2). These additional parameters were included as they are frequently used for object classification (Yamagata 1987; Heydon-Dumbleton et al. 1989).

In addition, the classifier sensitivity to object size was investigated by constructing classifiers for small (70–210 μm) and large (210–330 μm), as well as all object diameters.

Object magnitude is dependent on type; thus objects are binned by diameter, rather than magnitude. Performance was improved by training separate classifiers for small- and large-diameter ranges. The map is allowed to develop further specializations to cope with variations in the classification problem over the specific diameter range.

Different data presentation strategies were investigated to ensure that the classifier performance was not degraded by badly chosen input parameters or normalizations. As already discussed, SOMs are sensitive to input parameter scale. A 14×10 map was used for this optimization, an arbitrary choice but one that is required to reduce the map optimization problem to a manageable size.

As can be seen by considering the small and large classifiers shown in Table 2, different input strategies and map sizes produce the best results in each diameter range. Using the fuller input set produces comparable or slightly better results to those of the standard inputs, suggesting that the two additional input parameters do not provide contradictory information, and in some cases reinforce the map's learning.

For large objects the normalized input classifier produces marginally better average results (97.1 per cent for fully raw and 98.9 per cent for fully normalized), whereas for small

Table 2. Summary of self-organizing map classifiers.

Parameter	Small	Large
Map size and x,y dimensions	144 (36 × 4)	324 (27 × 13)
Variables	Fuller	Fuller
Data Normalisation	No	Yes

objects the raw input classifier gives a better average classification (92.8 per cent for fully raw and 89.1 per cent for fully normalized).

6 CLASSIFIER PARAMETER OPTIMIZATION

There are few theories concerning the applicability of different types of network to a given type of problem. Moreover, most networks have several free parameters that may be optimized. In the case of SOMs, the principal parameters are the overall size of the network and the ratio of the X and Y dimensions, the map aspect ratio. Optimization of these parameters for both the small and large classifiers was undertaken.

Faced with a large number of potential presentation and normalization strategies and map configurations, it is essential to restrict the number of optimization training runs if the CPU time required is to be kept to a manageable size. An artificial upper limit must be placed on maps size in order to produce a bounded optimization space. Thus a complete search of the parameter space is not possible and, as the aim of this work was to show that in principle such a classifier was able to separate stars and galaxies, the optimization described here was considered sufficient. A full classifier optimization, as outlined above, would be necessary if a complete object classification package were to be produced for use by astronomers.

7 CLASSIFIER PERFORMANCE

Using the optimized small- and large-diameter object maps, the overall best classifier performance was investigated. Object classification performance over given diameter ranges can be translated to a B-magnitude performance. The 70–330 μm diameter range corresponds to different stellar and galactic magnitude ranges; hence the classifier performance results are for different ranges for each object type, as can be seen in Fig. 1.

Fig. 1 shows the resulting classifier magnitude response. As outlined above the errors on the individual diameter band/magnitude classification rates may be quite significant. It is, however, interesting to note that the noise seen in the magnitude response curve appears less than that expected for a random error of 10 per cent. Fluctuations in the galaxy classification rate, which is dependent on a much smaller set of objects, are evident. For magnitudes greater than 18 a galaxy completeness of 95.3 per cent and contamination of 6.4 per cent is achieved to a magnitude of 20.3 for stars and 20.7 for galaxies. The magnitude limits are due to the data set object diameter size limit of 70 μm.

8 REDUCING THE NUMBER OF CALIBRATION OBJECTS

For a map containing a given number of nodes, the minimum number of calibration examples required is less than or equal to the number of nodes. During calibration the network looks for the object with the lowest classification error on a given node, and assigns to that node the class associated with the best-fitting object. Not all nodes need be associated with an object type; hence the user may not be required to classify an object for each node. In practice, there is no reason why the user should not be asked to classify the best-fitting objects during this phase of training. Thus, rather than having to classify several thousand objects, as is the case with the back-propagation classifer, only a few hundred would require classification. This represents a significant advantage, as training set classification requires a skilled observer and takes a great deal of time. For the combined classifier shown here the small- and large-object classifiers contained 144 and 324 nodes respectively; thus a maximum of 468 objects must be classified to train the system.

An alternative to calibrating objects is to use synthetic tracer objects. Such an approach has been used in a stellar classification application (Hernandez-Pajares, Floris & Murtagh 1994). Synthetic objects could be used for map calibration, rather than using real objects which best fitted each map node.

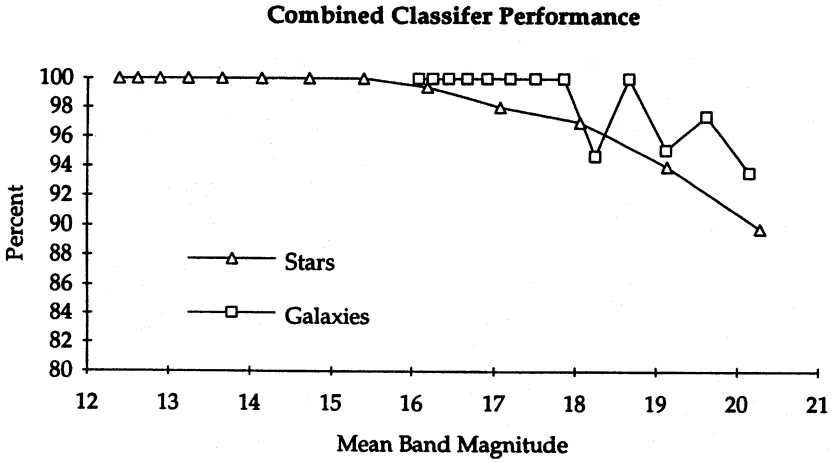

Figure 1. Overall magnitude performance for combined object classifier. A gradual reduction in classification accuracy is seen as the objects become fainter.

9 WEIGHT ANALYSIS

Although it is not possible to ascertain directly how the map classified any individual object, examination of the network weights can give some idea as to the relative significance of each input parameter. The small-object classifier, which is 36 × 4 map with 16 input parameters, has 2304 weights, 144 for each input. By examining the sum of the absolute values of the weights connected to each input, it is possible to quantify the emphasis placed on each input parameter.

Fig. 2 shows that the main weight emphasis is placed on the T_{av} and T_c parameters for the small-object classifier, whereas Fig. 3 shows that T_r and T_{cA} are by far the most important input parameters for the large-object classifier. This is not unreasonable, as other classification techniques have made extensive use of these parameter pairs. The difference in emphasis may be due to the large-object classifier using normalized inputs, whereas the small-object classifier does not.

In addition, the number of map nodes assigned to each object class is significant. Of the 144 nodes in the small-object map 80 are assigned to galaxies and 59 to stars, the remainder being unassigned. Nodes are assigned by searching a calibration set, in this case the training set, for the object with the smallest classification error on a given node. The associated object type is then assigned to that node. The distribution of assigned map nodes suggests that the map is better able to fit galaxy objects in the input space to the feature space mapping.

One might ask whether any of the other parameters are actually considered by the map when classifying objects. Small and large maps trained with just the two most emphasized parameters as inputs exhibit degraded classification performance when compared to the small and large maps with full inputs. The other input parameters must therefore be subtly altering the map classifications.

The overall classification rates are slightly reduced by restricting the number of input variables. The mean degradation figures of 1.0 per cent are, however, within the 1.6 per cent error of the combined classification rates, although a decreased performance trend of 1.0 per cent is seen in both small and large classifier maps.

Further work might consider the contribution of each input variable by training maps with combinations of inputs.

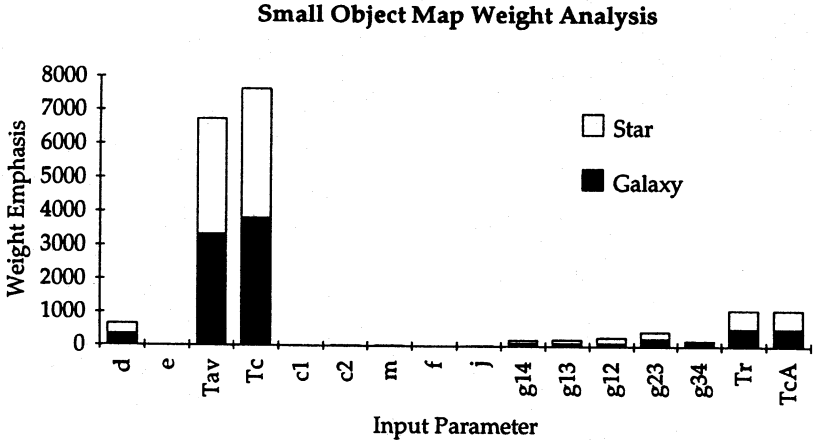

Figure 2. Weight analysis for small-object classifier map. The weighting is the sum of the absolute weights for each input parameter over the entire map. The weight denotes the emphasis of each input parameter on the final map classification.

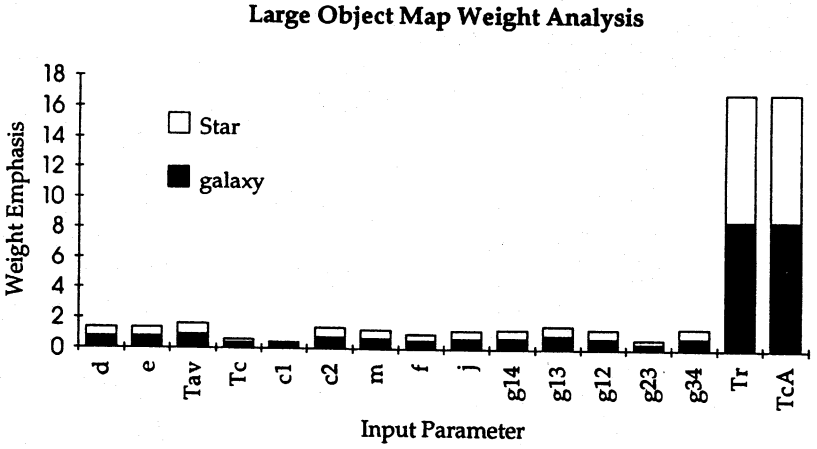

Figure 3. Weight analysis for large-object classifier map. The weighting is the sum of the absolute weights for each input parameter over the entire map. The weight denotes the emphasis of each input parameter on the final map classification.

Even when only using the two most emphasized inputs the map still constructs a non-linear decision boundary and so would be expected to produce better classifications than those based on a simple cut in a 2D parameter space.

10 COMPARISON WITH OTHER METHODS

The comparison of different classification methods has been hampered by differing the methodologies and data sets used. In this case, however, the classifier of Odewahn et al. (1992) was developed using the same data set, as was a rule-based tree algorithm developed by Murthy et al. (1993). A clear comparison of the two neural network approaches is therefore possible. A more general comparison with the techniques used by Murthy et al. is also discussed.

Here the back-propagation classifier is compared with the combined SOM classifier. It should be noted that both classifiers use the same data sets. The apparent increase in the magnitude of objects classified by the SOM is a feature of the diameter bins used. Both classifiers have a limiting magnitude of 20.3 for stars and 20.7 for galaxies, corresponding to an object diameter of 70 μm.

Figs 4 and 5 show that across the whole magnitude range the SOM produces a marginally better result, having an average completeness of 98.3 per cent and contamination of 1.5 per cent, compared to the back-propagation classifier which gives 96.2 and 2.0 per cent respectively. For faint objects, which for the purposes of galactic surveys are the more important, the SOM classifier produces a more complete sample. For magnitudes greater than 18 a completeness of 95.3 per cent and contamination of 6.4 per cent is achieved, compared to 92.0 and 3.2 per cent for the back-propagation classifier. Here the trade-off between completeness and contamination is illustrated. The SOM classifier achieves high completeness values at the expense of increased galaxy sample contamination. The overall classification accuracy is 94.4 per cent for both the SOM and back-propagation classifiers. When the random errors in the classifier results are taken into account, both classifiers must be said to produce similar results.

A more general comparison of various classification methods was undertaken by Murthy et al. (1993). These results are shown in Fig. 6 along with those for the back-propagation classifier of Odewahn et al. (1992) and the SOM classifier.

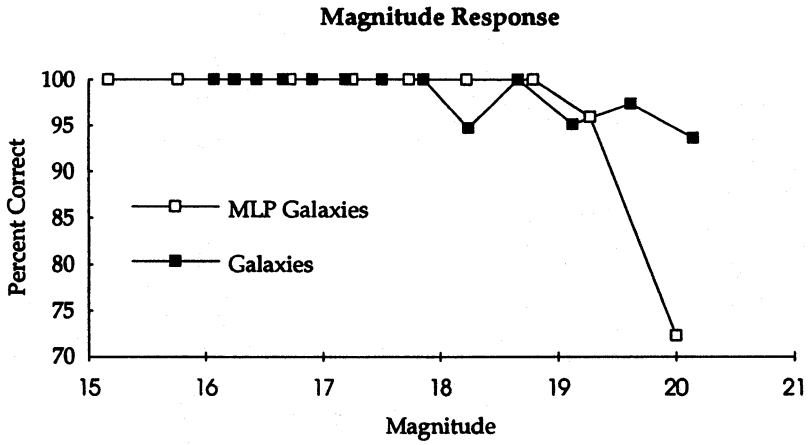

Figure 4. A comparison of the stellar magnitude responses for the supervised back-propagation classifier of Odewahn et al. (MLP galaxies) and the Kohonen SOM classifier described here (galaxies).

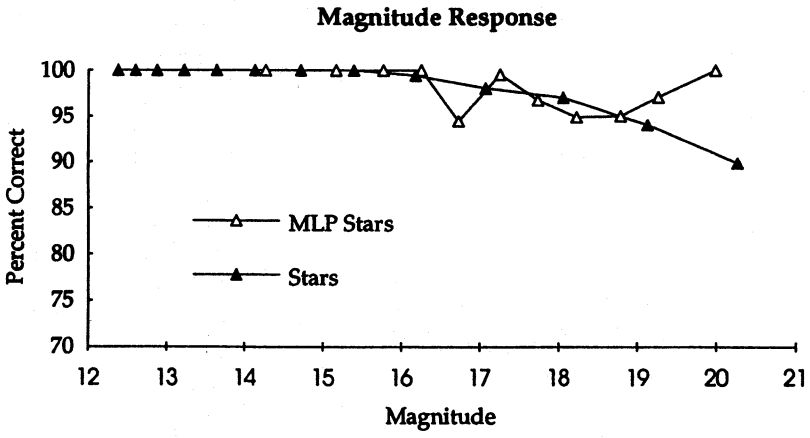

Figure 5. A comparison of the galactic magnitude responses for the supervised back-propagation classifier of Odewahn et al. (MLP stars) and the Kohonen SOM classifier described here (stars).

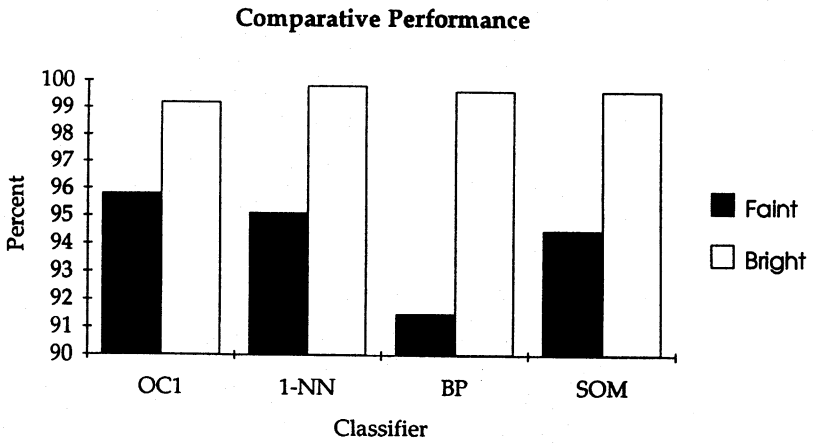

Figure 6. A comparison of several star/galaxy classification methods using the same data set for both faint (70–137 μm) and bright (> 137 μm) objects.

Fig. 6 shows the performance of the Randomized Multivariate Decision Tree of Murthy et al. (1993) – OC1, the 1st Nearest Neighbour classifier of Salzberg (1991) – 1NN, Odewahn et al.'s (1992) back-propagation network – BP and the SOM classifier discussed here – SOM.

All classifiers produce similar results for bright objects, with classifications accuracies in excess of 99 per cent. For faint objects the SOM outperforms the back-propagation classifier, which performs very badly for objects with magnitudes greater than 19. The SOM produces comparable performance to that of the nearest neighbour and decision tree classifiers, achieving a 94.4 per cent accuracy compared to 95.8 per cent for the decision tree.

11 CONCLUSIONS

The classifier discussed here achieves a similar performance to the classifiers developed by Odewahn et al. (1992) and Murthy et al. (1993). Both these other systems require a large number of objects, typically several thousand, to be manually classified for use as training data. The Kohonen SOM discussed requires a few hundred examples to be classified during the map calibratin phase of training. The SOM therefore achives similar classificatin accuracies to the other classifiers without the costly overhead of classifying large numbers of training set objects.

A more comprehensive data set is now required in order to assess fully the strengths and weaknesses of these different systems. The problem of plate-to-plate consistency must also be addressed, as classifiers must be able to work on plates taken under different seeing conditions. Work on plate-to-plate consistency has been undertaken by Odewahn & Nielson (1992) and shows that for the back-propagation classifier multiplate object classification is possible. A similar approach could also be used for the SOM classifier discussed here. For surveys containing highly variable plate collections the SOM approach may offer a significant advantage because of the small number of objects which require manual classification when training a classifier.

ACKNOWLEDGMENTS

ASM was funded by a SERC research studentship. Dr Kevin Bennett is thanked for his comments on the resulting thesis, and Dr Laurence Jones for his comments on the chapter which led to this paper. We are particularly grateful to Steve Odewahn for providing the POSS plate data and classified objects. The GNU Free Software Foundation Inc., USA, provided numerous UNIX applications and Teuvo Kohonen produced the neural net software used by the authors. The SOMPAK (version 1.2) Public Domain SOM simulation package, developed by Teuvo Kohonen and others, was used for all the star/galaxy classification work. SOKPAK 3.1 is available by anonymous ftp from lvq@cochlea.hut.fi.

REFERENCES

Boyle B. J., 1991, in Barrow J. D., Mestel L., Thomas P. A., eds, Proc. Texas ESO-CERN Symposium on Relativistic Astrophysics, Cosmology and Fundamental Physics, The Quasar Population at High Redshifts. Brighton, England, p. 14
Broadhurst T. J., Ellis R. S., Shanks T., 1988, MNRAS, 235, 827
Charlier C. V. L., 1922, Ark. Math. Astr. Fys., 16, 22
Corwin H. G., de Vaucouleurs G., de Vaucouleurs A., 1985, Southern Sky Catalog. Univ. of Texas Astronomy Dept.
Ellis R., 1987, in Hewitt et al., eds, IAU Symp. 136, Observational Cosmology. Reidel, Dordrecht, p. 367
Godwin J. G., Metcalfe N., Peach J. V., 1983, MNRAS, 202, 113
Hancock P. J. B., 1988, in Proc. Connectionist Models Summer School, Data Representation in Neural Nets: an Empirical Study. Morgan Kaufmann, Pittsburgh, PA, p. 11
Hernandez-Pajares M., Floris J., Murtagh F., 1994, Vistas Astron., 36, 317
Heydon-Dumbleton N. H., Collins C. A., MacGillivray H. T., 1989, MNRAS, 238, 379
Hopfield J. J., Tank D. W., 1986, Science, 223, 625
Jolliffe I. T., 1986, Principal Component Analysis. Springer-Verlag, NY
Kohonen T., 1990, IEEE Proc., 78, 1464

Kohonen T., Kangas J., Laaksonen J., 1992, SOMPAK, The Self Organising Map Program Package, version 1.2. Helsinki Univ. of Technology, Computer and Information Science Lab., Helsinki, Finland, available by anonymous ftp from cochlea.hut.fi:/pub/sompak

Kron R., 1982, Vistas Astron., 26, 37

Lahav O., 1994, Vistas Astron., 36, 251

Maddox S. J., Efstathiou G., Sutherland W. J., Loveday J., 1990, MNRAS, 243, 692

Miller A. S., 1993, Vistas Astron., 36, 141

Murthy S. K., Kasif S., Salzberg S., Beigel R., 1993, OC1: A Randomised Algorithm for Building Oblique Decision Trees. Proceedings of the Eleventh National Conference on Artificial Intelligence. Morgan Kaufmann, Washington, DC

Odewahn S. C., Nielson M. L., 1994, Vistas Astron., 36, 281

Odewahn S. C., Stockwell E. B., Pennington R. L., Humphreys R. M., Zumach W., 1992, 103, 318

Rumelhart D. E., Hinton G. E., McClelland J. L., 1986, in Rumelhart D. E., McClelland J. L., The PDP Research Group, eds, Parallel Distributed Processing: Explorations in the Microstructure of Cognition, Vol. 1, Foundations. MIT Press, Cambridge, MA, p. 45

Salzberg S., 1991, in Methodologies for Intelligent Systems: 6th International Symposium, Distance Metrics for Instance Based Machine Learning. ISMIS '91, p. 399

Serra-Ricart M., Garrido L., Gaitan V., 1994, Vistas Astron., 36, 257

Weir N., Djorgovski S., Fayyad U., Roden J., Rouquette N., 1992, in Heck A., Murtagh F., eds, Proc. Astronomy from Large Databases II, SKICAT: A System for the Scientific Analysis of the Palomar-STScI Digital Sky Survey. Haguenau, France, p. 513

Widrow B., Lehr M. A., 1990, Proc. IEEE, 78, 1415

Yamagata T., 1987, Optimum Parameters for the Discrimination of the Images between Galaxies and Stars. Univ. Tokyo, preprint

Zwicky F., Herzog E., Kowal C. T., Wild P., Karpowicz M., 1961–68, Catalog of Galaxies and of Clusters of Galaxies. California Institute of Technology, Pasadena